BAMS Supplement

Studying Urban Climate and Air Quality in the Alps

The Innsbruck Atmospheric Observatory

Thomas Karl, Alexander Gohm, Mathias W. Rotach, Helen C. Ward, Martin Graus, Alexander Cede, Georg Wohlfahrt, Albin Hammerle, Maren Haid, Martin Tiefengraber, Christian Lamprecht, Johannes Vergeiner, Axel Kreuter, Jochen Wagner, and Michael Staudinger

https://doi.org/10.1175/BAMS-D-19-0270.2
Corresponding author: Thomas Karl, thomas.karl@uibk.ac.at
This document is a supplement to https://doi.org/10.1175/BAMS-D-19-0270.1

In final form 12 December 2019

Flux footprint

Figure ES1 depicts the land-cover distribution of the urban flux footprint as described in the main body of the manuscript.

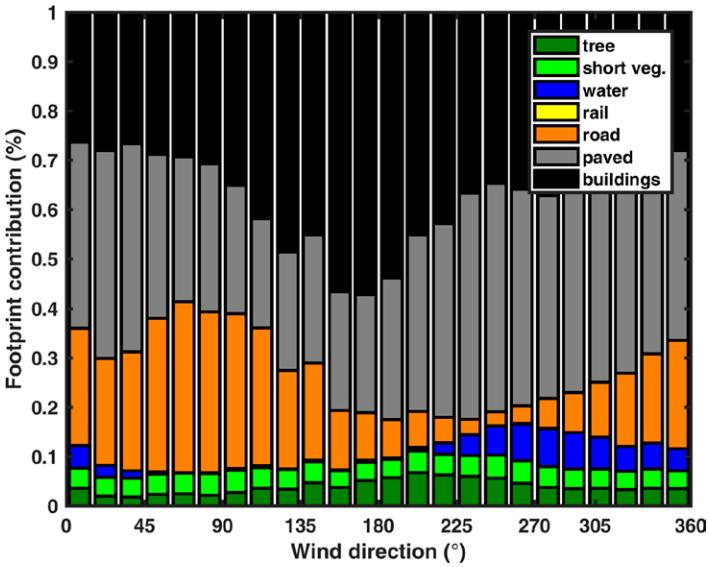

Fig. ES1. Land surface contribution to the IAO flux footprint as a function of wind direction. Data represent the year 2018.

Iao core instrumentation

Micrometeorology. Instruments are installed on a lattice mast at the southeast end of the university building roof (Fig. ES2), giving a measurement height of 9.5 m above the rooftop and 42.8 m above ground level. A sonic anemometer and closed-path infrared gas analyzer (CPEC200, Campbell Scientific Ltd.) provide high-frequency (10 Hz) measurements of the three components of wind speed (u, v, w; Fig. ES3), sonic temperature, and mixing ratios of water vapor and carbon dioxide. Incoming and outgoing shortwave ($K_{\downarrow}$, $K_{\uparrow}$) and longwave ($L_{\downarrow}$, $L_{\uparrow}$) radiation are measured by a four-component net radiometer (CNR4, Kipp and Zonen) and temperature and relative humidity are also measured (HC2S3, Campbell Scientific). It is planned that additional instrumentation will be added to the Innsbruck Atmospheric Observatory (IAO) tower and at lower levels to form a profile that extends down into the street canyon. Data have been collected from the IAO tower since May 2017. From 2015 to 2016 data were collected using a similar set up on the northeast side of the roof (at a distance of 49 m from the IAO tower).

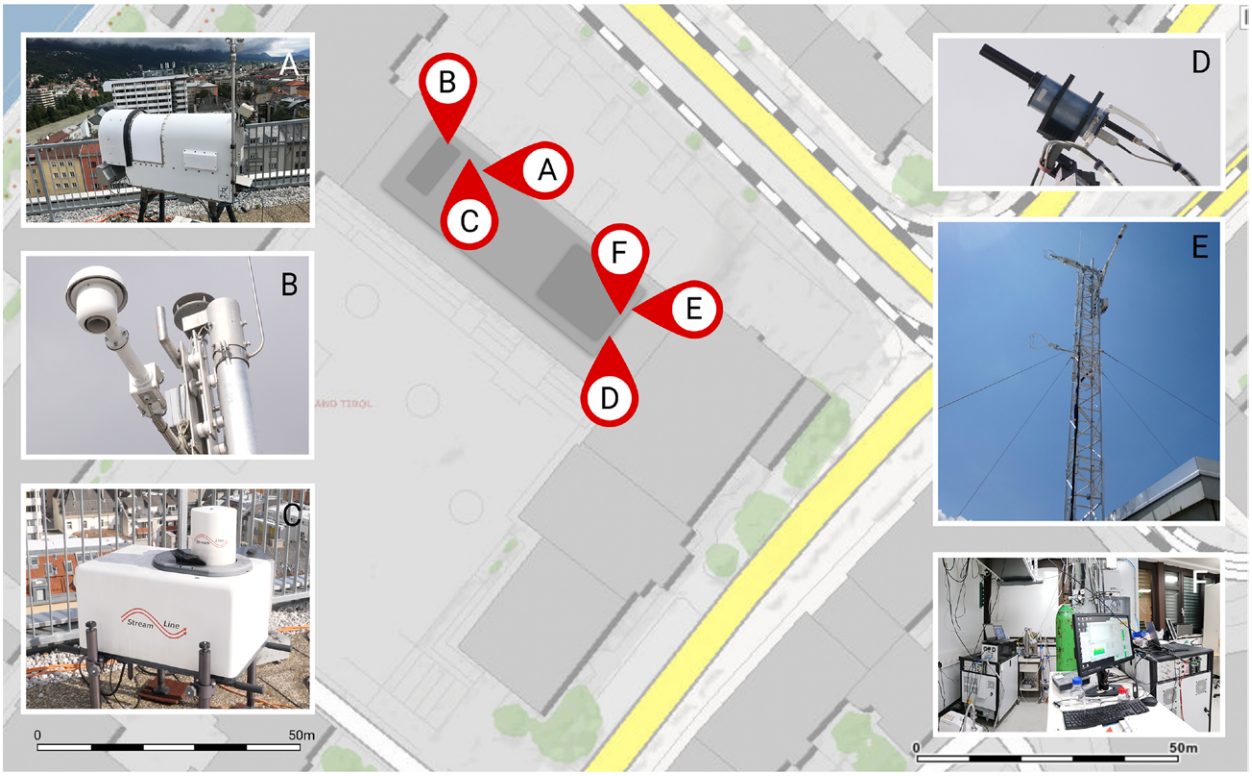

Fig. ES2. Top view of the IAO facilities: (a): microwave sounder, (b) TAWES weather station, (c) Doppler wind lidar system, (d) Pandora, (e) flux tower, and (f) laboratory facilities. Map data obtained from Land Tirol (TIRIS).

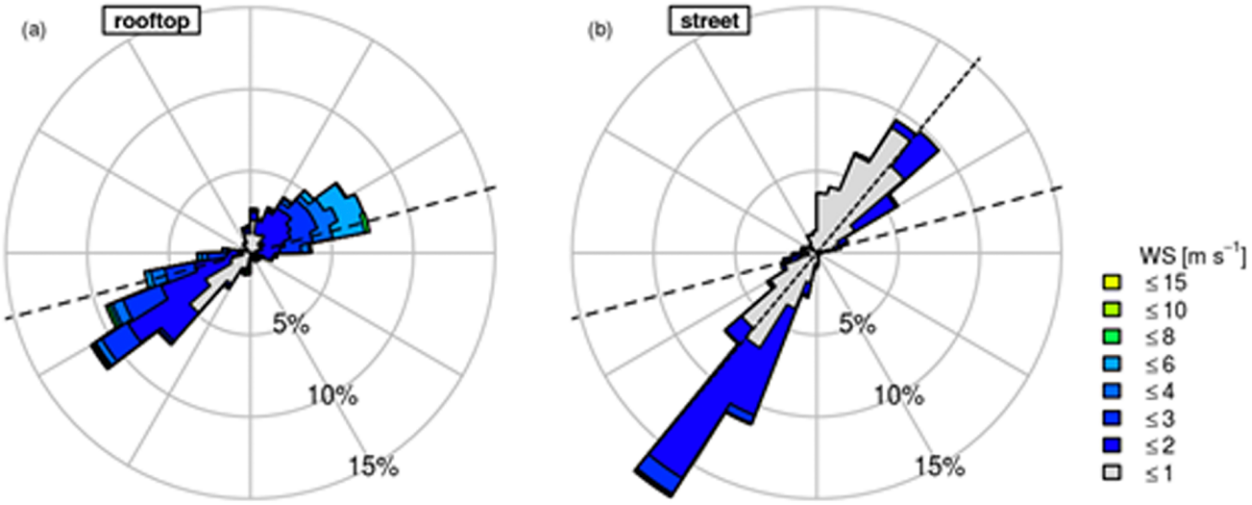

Fig. ES3. Wind roses for (a) IAO rooftop and (b) street canyon station for August 2018. The dashed lines mark the orientation of the Inn Valley and the dotted line in (b) marks the direction of the street.

The previous tower was collocated with the Teilautomatisches-Wetter-Erfassungs-System (TAWES), Universität Innsbruck, operated by Austrian National Weather Service (ZAMG) as part of the WMO Centennial Observing Station network. Figure ES2 shows a detailed view of the rooftop where most of the instruments are located. Next to the flux tower, the IAO chemistry and physics laboratory provides approximately 65 m^2 of indoor space, where most of the atmospheric chemistry measurements are performed (Table ES1). The laboratory space is close to the tower, so that micrometeorological measurements of various chemical species can be conducted. Due to the proximity of the tower, flexible installations for instrumentation that needs to be housed inside and requires short access sampling ports to the outside are possible. For closed path instruments sample air is pumped from near the sonic anemometer at the top of the flux mast through a 13 m long Teflon inlet line with 6.35 mm inner diameter at a rate of circa 19 liter per minute at standard temperature and pressure (slpm) resulting in a residence time of approximately 0.4 s. The inlet system is pressure and temperature stabilized and covered by an insulation sleeve, which also keeps the tubing dark. A valve manifold distributes subsamples to various gas analyzers; the gas flow rate through the inlet line is constant irrespective of the sampling rates and the number of instruments subsampling from

Table ES1. Trace gas instrumentation of the IAO laboratory from 2019.

Instrument	Manufacturer	Technique	Parameter	Measurement rate
EC155 closed-path CO_2/H_2O gas analyzer	Campbell	Infrared absorption spectroscopy	CO_2, H_2O	10 Hz
CLD899	Ecophysics	Chemiluminescence	NO_x, NO_2, NO	5 Hz
LG Cavity Ringdown	Los Gatos	UV absorption spectroscopy	NO_2	5 Hz
Fast Ozone Analyzer	Sextant Technology	Chemiluminescence	O_3	10 Hz
APOA-360	Horiba	UV absorption spectroscopy	O_3	5 s
APMA-360	Horiba	Infrared absorption spectroscopy	CO	5 s
PTR-QiTOF	Ionicon	Chemical ionization mass spectrometer	NMVOC	10 Hz
PTR-TOF6000 × 2	Ionicon	Chemical ionization mass spectrometer	NMVOC, organic aerosol (PM1)	10 Hz or 1 min for organic aerosols

the manifold. Currently the air-conditioned laboratory provides about 50 kW of power. All electrical and data connections leading to the outside are electrically insulated and secured by a lightning protection system. The IAO is situated close to three EU accredited air quality (AQ) stations, operated by the national air quality network (EU-ID: AT72110; 577 m MSL; longitude: 11°23′32.5″, latitude: 47°15′45.4″; EU-ID: AT72106; 570 m MSL; longitude: 11°25′1.0″, latitude: 47°16′16.6″; EU-ID AT72113: 678 m MSL; 11°22′28.8″ 47°16′11.7″). It is anticipated that various synergies between activities at the IAO and AQ measurements (Table ES3) at these stations will develop over time.

In situ chemistry. In situ observations of NO_x, NO, NO_2, O_3, CO_2, and CO are performed on a continuous basis. With the exception of CO the above gases are measured fast enough to perform eddy covariance (e.g., 5–10 Hz sampling resolution). NO_x and NO are measured using an Ecophysics CLD899 two-channel chemiluminescence analyzer in 5 Hz mode. The instrument allows NO_2 to be derived by difference. In addition NO_2 is also directly measured using a Los Gatos cavity-ringdown absorption spectrometer (λ = 405 nm) (Brent et al. 2013; Castellanos et al. 2009; Hargrove et al. 2006; O'Keefe and Deacon 1988; Osthoff et al. 2006). The O_3 is measured 10 Hz by a Fast Ozone Analyzer from Sextant Technology Ltd., New Zealand. It is based on a chemiluminescence reaction between O_3 and a coumarin target. To derive ozone mixing ratios another slow-response (5 s) but absolute measuring nondispersive ultraviolet absorption instrument (APOA-360, Horiba, Japan) is operated in parallel (Muller et al. 2010). CO is obtained from a nondispersive infrared analysis instrument and logged every 5 s (APMA-360, Horiba). CO_2 and H_2O fluxes and concentrations are obtained from a EC155 closed-path infrared gas analyzer as part of the CPEC 200 system mentioned above (Campbell Scientific, United States). Nonmethane volatile organic compounds (NMVOC) are measured by proton-transfer-reaction mass spectrometry (Hansel et al. 1995; De Gouw et al. 2003; Yuan et al. 2017; Norman et al. 2009). Proton-transfer-reaction mass spectrometry (PTR-MS) is a fast technique for the quantitative measurement of most VOCs and a few inorganic trace gases in the atmosphere. It allows for the identification of hundreds of mass peaks corresponding to VOCs from a multitude of source categories in urban environments and enables the quantification of mixing ratios as well as turbulent fluxes of these compounds (Karl et al. 2018). The IAO has at its disposal a PTR quadrupole-interface time-of-flight mass spectrometer (PTR-QiTOF; Ionicon Analytik; for details, see Sulzer et al. 2014) with a switchable reagent ion source (SRI; details, see Jordan et al. 2009). The operation of the SRI in H_3O+ mode enables the quantification of all detected VOCs—even those that have not been calibrated for—at low error margins because proton transfer proceeds near collisional rate and the reaction rate coefficients for different VOCs are within a range of ±40% around 2.8×10^{-9} cm^3 s^{-1}. Ionization with NO+ is more selective allowing the separation of isomers; it is also softer reducing fragmentation of product ions. Regardless of the ionization method mass spectral information is collected at 10 Hz allowing for the calculation of the turbulent vertical flux of VOCs. Since 2019 the pool of analytical instrumentation of the IAO also comprises a PTR-TOF6000 × 2 with a chemical analysis of aerosol online

Table ES2. Summary of technical specifications of the IAO Halo Photonics Doppler wind lidars.

Parameter	SL88	SLXR142
Wavelength	1.5 μm	1.5 μm
Pulse repetition frequency	15 kHz	10 kHz
FFT length	1,024	2,048
Velocity resolution	0.038 m s^{-1}	0.038 m s^{-1}
Nyquist velocity	19.4 m s^{-1}	38.7 m s^{-1}
Laser pulse length (FWHM)	175 ns	380 ns
Receiver sampling frequency	50 MHz	100 MHz
Unambiguous range	10 km	15 km
Range gate length	Selectable from 18 to 60 m	Selectable from 18 to 120 m

(CHARON; Ionicon Analytik) interface for the chemical characterization of semivolatile submicron particles (Eichler et al. 2015; Müller et al. 2017). The CHARON interface collimates the aerosol into a narrow particle beam enhancing the particle mass concentration in a subsample from the center of the gas and particle stream by a factor of 25–40. The aerosol is continuously evaporated and the semivolatile fraction is analyzed by the PTR-TOF system. For the organic and nitrate fraction of aerosol Müller et al. (2017) found reasonable agreement with a cosampling aerosol mass spectrometer (AMS; Aerodyne Research Inc.). The PTR-TOF6000 × 2 is equipped with an SRI, an ion funnel and a hexapole ion guide. It can be operated both in aerosol mode as well as VOC mode (equivalent to the PTR-QiTOF). In aerosol mode spectra are integrated over 10 s whereas in VOC mode the instrument has full eddy covariance capability. More detailed information on in situ measurements is provided in Table ES4.

Table ES3. List of intensive operational phases (IOPs) presented in this article.

IOP	Date	Objectives
IOP2015	1 Jul–30 Oct 2015	Test campaign to perform first urban flux measurements of trace gases, heat, and momentum fluxes
IOP2018	31 Jul–15 Sep 2018	Urban air quality campaign focused on urban exchange processes with a focus on regulated urban pollutants during summer

Remote sensing—Composition. Two spectrometer systems (Pandora) are operated directly on the roof of the IAO building. Pandora is a ground-based remote sensing UV–visible spectrometer capable of performing measurements in direct sun, direct moon and multiaxes sky observation modes (see, e.g., Herman et al. 2009; Knepp et al. 2013; Zhao et al. 2019). The two Pandoras at the IAO are also part of the worldwide operating Pandonia Global Network, which has been established to provide homogenized measurements used for air quality monitoring and satellite validation (http://pandonia-global-network.org). This network produces operational data products such as total NO_2 and O_3 column amounts, as well as a series of research data products such as surface concentrations, total and tropospheric column amounts of different trace gases (O_3, NO_2, SO_2, HCHO, etc.). The sampling rate varies somewhat for different output products, but is 10 min or shorter for all. Column aerosol information is retrieved via sun photometry from a 4 channel (368, 412, 501, and 862 nm) Precision Filter Radiometer (PFR) (developed for the WMO Global Atmospheric Watch aerosol network at the Physikalisch-Meteorologisches Observatory Davos, Switzerland). Highly accurate time series of aerosol optical depth (AOD) and Ångström parameter α with a 1 min time resolution are available already since 2007 (Wuttke et al. 2012).

Remote sensing—Meteorology. Active remote sensing is performed at the IAO with two scanning Doppler wind lidars manufactured by Halo Photonics: a Streamline system (SL88) available since August 2014 and a Streamline XR system with extended range (SLXR142) since September 2017. Both are 1.5-mm pulsed Doppler wind lidars developed to observe wind velocities and aerosol backscatter intensities in the atmospheric boundary layer (Pearson et al. 2009). Technical specifications are summarized in Table ES2. We typically use a range gate length of between 18 and 36 m and an accumulation time per ray of 1 s. The SL88 has been used since its first installation at the IAO rooftop to continuously measure the vertical profile of the horizontal winds by applying the velocity–azimuth display (VAD) analysis technique to the line-of-sight velocities gathered by 8 rays with different azimuth angles (45° spacing) at a constant elevation of 70°. Since fall 2017 we use a different scan pattern: the so-called six-beam method (Sathe et al. 2015) to deduce turbulence quantities in addition to the mean wind profiles that are still derived with the VAD technique. The lidar system has also been operated as a mobile system during dedicated measurement campaigns. Passive remote sensing of the vertical thermodynamic structure of the atmosphere is performed at the IAO with

a humidity and temperature profiler (HATPRO) manufactured by RPG Radiometer Physics since September 2012. HATPRO is a microwave radiometer operating in two frequency bands, each comprising 7 channels, for humidity (22–31 GHz) and temperature (51–58 GHz) profiling, respectively (Rose et al. 2005). Besides vertical profiles, integrated humidity measures such as liquid water path (LWP) and integrated water vapor (IWV) are retrieved as described by Massaro et al. (2015). HATPRO is operated in two alternating modes: the zenith-pointing mode and the elevation-scanning mode (where the elevation angle changes from about 4° to 90°). The latter is used to enhance the resolution of the temperature profile in the ABL.

Table ES4. Isobaric formulas of NMVOCs detected by PTR-QiTOFMS at the IAO.

Sum formula	Ionic mass (=molecular weight + 1 proton)	24 h mean concentration (ppbv)	24 h maximum concentration (ppbv)
CH2O	31.0178	0.2052	0.5293
CH4O	33.0335	5.5808	15.5847
C3H4	41.0386	0.2521	1.5316
C2H3N	42.0338	0.1201	0.4664
C2H2O	43.0178	0.6531	3.0337
C3H6	43.0542	0.7299	5.405
C2H4O	45.0335	0.9602	4.5512
CH2O2	47.0128	0.3746	1.5627
C2H6O	47.0491	0.8112	4.2183
CH4S	49.0106	0.0078	0.0291
CH4O2	49.0284	0.0077	0.0372
CH6ON	49.0522	0.0027	0.0135
C3H3N	54.0338	0.0029	0.025
C3H4O	57.0335	0.1108	0.401
C4H8	57.0699	1.772	33.5985
C3H6O	59.0491	2.825	16.1678
C4H10	59.0855	0.0532	0.2227
C2H4O2	61.0284	0.957	7.3425
C3H8O	61.0648	0.0231	0.1168
C2H6S	63.0263	0.0321	0.1435
C2H6O2	63.0441	0.0289	0.2516
C5H6	67.0542	0.0147	0.0445
C4H4O	69.0335	0.0209	0.0986
C5H8	69.0699	0.1651	0.6064
C4H6O	71.0491	0.2212	0.7684
C5H10	71.0855	0.1521	0.8228
C3H4O2	73.0284	0.1077	0.9999
C4H8O	73.0648	0.3316	3.6623
C3H6O2	75.0441	0.2949	0.9854
C2H4O3	77.0233	0.1326	0.7204
C3H8O2	77.0597	0.0308	0.1318
C2H6O3	79.039	0.0476	0.1975
C6H6	79.0542	0.1226	0.4065
C5H4O	81.0335	0.0187	0.0763
C6H8	81.0699	0.0999	0.5178
C4H2O2	83.0128	0.0079	0.0381

Table ES4. Continued.

Sum formula	Ionic mass (=molecular weight + 1 proton)	24 h mean concentration (ppbv)	24 h maximum concentration (ppbv)
C5H6O	83.0491	0.0383	0.1364
C6H10	83.0855	0.1307	0.4633
C4H4O2	85.0284	0.0332	0.1007
C5H8O	85.0648	0.0511	0.1689
C6H12	85.1012	0.0664	0.2572
C4H6O2	87.04	9.19×10^{-2}	3.31×10^{-1}
C5H10O	87.08	6.55×10^{-2}	2.24×10^{-1}
C3H4O3	89.02	3.40×10^{-2}	3.76×10^{-1}
C4H8O2	89.06	1.70×10^{-1}	4.65×10^{0}
C3H6O3	91.04	2.95×10^{-2}	1.27×10^{-1}
C7H6	91.05	5.30×10^{-2}	4.04×10^{-1}
C7H7	92.06	1.14×10^{-2}	4.12×10^{-2}
C6H4O	93.03	3.85×10^{-2}	1.88×10^{-1}
C7H8	93.07	3.01×10^{-1}	1.80×10^{0}
C6H6O	95.05	1.97×10^{-2}	6.83×10^{-2}
C7H10	95.09	3.08×10^{-2}	9.96×10^{-2}
C5H4O2	97.03	2.53×10^{-2}	1.23×10^{-1}
C6H8O	97.0648	0.0246	0.0891
C7H12	97.1012	0.0493	0.1595
C4H2O3	99.0077	0.0192	0.0721
C5H6O2	99.0441	0.0582	0.1856
C6H10O	99.0804	0.0484	0.1778
C7H14	99.1168	0.0092	0.0379
C4H4O3	101.0233	0.0403	0.338
C5H8O2	101.0597	0.1098	2.624
C6H12O	101.0961	0.0371	0.2528
C4H6O3	103.039	0.022	0.0777
C5H10O2	103.0754	0.0178	0.0545
C4H8O3	105.0546	0.0181	0.0547
C8H8	105.0699	0.0224	0.0751
C7H6O	107.0491	0.0518	0.2251
C8H10	107.0855	0.258	1.5652
C6H4O2	109.0284	0.0072	0.0223
C7H8O	109.0648	0.0163	0.085
C8H12	109.1012	0.0323	0.1238
C6H6O2	111.0441	0.0145	0.0528
C7H10O	111.0804	0.0239	0.0998
C8H14	111.1168	0.0308	0.1092
C5H4O3	113.0233	0.0221	0.1057
C6H8O2	113.0597	0.0323	0.1018
C7H12O	113.0961	0.0164	0.0577
C8H16	113.1325	0.0057	0.0225
C5H6O3	115.039	0.0224	0.0736
C6H10O2	115.0754	0.0392	0.1131
C7H14O	115.1117	0.0172	0.0552

Table ES4. Continued.

Sum formula	Ionic mass (=molecular weight + 1 proton)	24 h mean concentration (ppbv)	24 h maximum concentration (ppbv)
C4H4O4	117.0182	0.004	0.0165
C5H8O3	117.0546	0.015	0.0719
C6H12O2	117.091	0.025	0.373
C4H6O4	119.0339	0.0047	0.0205
C9H10	119.0855	0.0107	0.0543
C8H8O	121.0648	0.0169	0.0929
C9H12	121.1012	0.1136	0.5808
C2H3O5N	122.0084	0.0038	0.0126
C7H6O2	123.0441	0.0107	0.0326
C8H10O	123.0804	0.0105	0.0359
C9H12	123.1168	0.0254	0.0975
C7H8O2	125.0597	0.0128	0.0394
C8H12O	125.0961	0.0174	0.0574
C9H16	125.1325	0.0174	0.0888
C6H6O3	127.039	0.0096	0.0295
C7H10O2	127.0754	0.0232	0.0658
C8H14O	127.1117	0.0133	0.0412
C9H18	127.1481	0.0038	0.0116
C6H8O3	129.0546	0.0193	0.0916
C10H8	129.0699	0.0354	0.1656
C7H12O2	129.091	0.0237	0.1317
C8H16O	129.1274	0.0133	0.0761
C5H6O4	131.0339	0.0051	0.0203
C6H10O3	131.0703	0.0097	0.0348
C7H14O2	131.1067	0.0067	0.0225
C9H8O	133.0648	0.0072	0.052
C10H12	133.1012	0.014	0.1399
C8H6O2	135.0441	0.0058	0.0199
C9H10O	135.0804	0.0195	0.0738
C10H14	135.1168	0.0666	0.232
C8H8O2	137.0597	0.0138	0.0518
C9H12O	137.0961	0.0383	0.1568
C10H16	137.1325	0.0757	0.3699
C7H6O3	139.039	0.0104	0.0335
C8H10O2	139.0754	0.0315	0.1154
C9H14O	139.1117	0.0769	0.3199
C7H8O3	141.0546	0.0134	0.0503
C8H12O2	141.091	0.0174	0.0588
C9H16O	141.1274	0.0102	0.0676
C6H6O4	143.0339	0.0051	0.0152
C7H10O3	143.0703	0.0152	0.0432
C8H14O2	143.1067	0.0187	0.0702
C9H18O	143.143	0.0202	0.2557
C6H8O4	145.0495	0.005	0.0211
C7H12O3	145.0859	0.0054	0.0183

Table ES4. Continued.

Sum formula	Ionic mass (=molecular weight + 1 proton)	24 h mean concentration (ppbv)	24 h maximum concentration (ppbv)
C8H16O2	145.1223	0.0054	0.0188
C9H6O2	147.0441	0.0092	0.1401
C11H14	147.1168	0.0069	0.0408
C8H4O3	149.0233	0.004	0.015
C10H12O	149.0961	0.0094	0.0355
C11H16	149.1325	0.0093	0.057
C10H14O	151.1117	0.0737	0.3737
C11H18	151.1481	0.013	0.0548
C8H8O3	153.0546	0.0163	0.0557
C9H12O2	153.091	0.0279	0.1152
C10H16O	153.1274	0.0411	0.1393
C11H20	153.1638	0.0074	0.025
C9H14O2	155.12	0.0356	0.1129
C11H8O	157.12	0.0355	0.0955
C11H10O	159.12	0.0148	0.0506
C10H8O2	161.12	0.0093	0.034
C11H14O	163.12	0.0112	0.0572
C10H12O2	165.12	0.0127	0.0436
C9H10O3	167.0703	0.0066	0.0205
C10H14O2	167.1067	0.015	0.0616
C12H22	167.1794	0.002	0.007
C8H8O4	169.0495	0.0062	0.0236
C9H12O3	169.0859	0.0173	0.0708
C10H16O2	169.1223	0.0421	0.2323
C11H20O	169.1587	0.0079	0.0347
C12H24	169.1951	0.0032	0.017
C11H18O2	183.16	0.0149	0.0448
C11H20O2	185.1587	0.018	0.0632
C12H14O2	191.1587	0.0054	0.0274
C15H22	203.1794	0.0024	0.0083
C15H24	205.1951	0.004	0.0196
C6H28O3Si3	223.0637	0.0009	0.0035
C8H24O4Si4	297.0824	0.0005	0.0019
C9H27O5Si5	355.0699	0.0017	0.0068
C10H30O5Si5	371.1012	0.0031	0.0156
C12H36O6Si6	445.12	0.0002	0.0011
C13H42O7Si7	519.1388	0.0002	0.0002

References

Brent, L. C., and Coauthors, 2013: Evaluation of the use of a commercially available cavity ringdown absorption spectrometer for measuring NO_2 in flight, and observations over the mid-Atlantic states, during DISCOVER-AQ. *J. Atmos. Chem.*, **72**, 503–521, https://doi.org/10.1007/s10874-013-9265-6.

Castellanos, P., W. T. Luke, P. Kelley, J. W. Stehr, S. H. Ehrman, and R. R. Dickerson, 2009: Modification of a commercial cavity ring-down spectroscopy NO_2 detector for enhanced sensitivity. *Rev. Sci. Instrum.*, **80**, 113107, https://doi.org/10.1063/1.3244090.

De Gouw, J., C. Warneke, T. Karl, G. Eerdekens, C. Van der Veen, and R. Fall, 2003: Sensitivity and specificity of atmospheric trace gas detection by proton-transfer-reaction mass spectrometry. *Int. J. Mass Spectrom.*, **223–224**, 365–382, https://doi.org/10.1016/S1387-3806(02)00926-0.

Eichler, P., M. Müller, B. D'Anna, and A. Wisthaler, 2015: A novel inlet system for online chemical analysis of semi-volatile submicron particulate matter. *Atmos. Meas. Tech.*, **8**, 1353–1360, https://doi.org/10.5194/amt-8-1353-2015.

Hansel, A., A. Jordan, R. Holzinger, P. Prazeller, W. Vogel, and W. Lindinger, 1995: Proton transfer reaction mass spectrometry: On-line trace gas analysis at the ppb level. *Int. J. Mass Spectrom. Ion Processes*, **149–150**, 609–619, https://doi.org/10.1016/0168-1176(95)04294-U.

Hargrove, J., L. Wang, K. Muyskens, M. Muyskens, D. Medina, S. Zaide, and J. Zhang, 2006: Cavity ring-down spectroscopy of ambient NO_2 with quantification and elimination of interferences. *Environ. Sci. Technol.*, **40**, 7868–7873, https://doi.org/10.1021/es061287o.

Herman, J., A. Cede, E. Spinei, G. Mount, M. Tzortziou, and N. Abuhassan, 2009: NO_2 column amounts from ground-based Pandora and MFDOAS spectrometers using the direct-sun DOAS technique: Intercomparisons and application to OMI validation. *J. Geophys. Res.*, **114**, D13307, https://doi.org/10.1029/2009JD011848.

Jordan, A., and Coauthors, 2009: An online ultra-high sensitivity proton-transfer-reaction mass-spectrometer combined with switchable reagent ion capability (PTR-SRI-MS). *Int. J. Mass Spectrom.*, **286**, 32–38, https://doi.org/10.1016/j.ijms.2009.06.006.

Karl, T., M. Striednig, M. Graus, A. Hammerle, and G. Wohlfahrt, 2018: Urban flux measurements reveal a large pool of oxygenated volatile organic compound emissions. *Proc. Natl. Acad. Sci. USA*, **115**, 1186–1191, https://doi.org/10.1073/pnas.1714715115.

Knepp, T., and Coauthors, 2013: Estimating surface NO_2 and SO_2 mixing ratios from fast-response total column observations and potential application to geostationary missions. *J. Atmos. Chem.*, **72**, 261–286, https://doi.org/10.1007/s10874-013-9257-6.

Massaro, G., I. Stiperski, B. Pospichal, and M. W. Rotach, 2015: Accuracy of retrieving temperature and humidity profiles by ground-based microwave radiometry in truly complex terrain. *Atmos. Meas. Tech.*, **8**, 3355–3367, https://doi.org/10.5194/amt-8-3355-2015.

Muller, J. B. A., C. J. Percival, M. W. Gallagher, D. Fowler, M. Coyle, and E. Nemitz, 2010: Sources of uncertainty in eddy covariance ozone flux measurements made by dry chemiluminescence fast response analysers. *Atmos. Meas. Tech.*, **3**, 163–176, https://doi.org/10.5194/amt-3-163-2010.

Müller, M., P. Eichler, B. D'Anna, W. Tan, and A. Wisthaler, 2017: Direct sampling and analysis of atmospheric particulate organic matter by proton-transfer-reaction mass spectrometry. *Anal. Chem.*, **89**, 10889–10897, https://doi.org/10.1021/acs.analchem.7b02582.

Norman, M., and Coauthors, 2009: Intercomparison of ammonia measurement techniques at an intensively managed grassland site (Oensingen, Switzerland). *Atmos. Chem. Phys.*, **9**, 2635–2645, https://doi.org/10.5194/acp-9-2635-2009.

O'Keefe, A., and D. A. G. Deacon, 1988: Cavity ring-down optical spectrometer for absorption measurements using pulsed laser sources. *Rev. Sci. Instrum.*, **59**, 2544–2551, https://doi.org/10.1063/1.1139895.

Osthoff, H. D., and Coauthors, 2006: Measurement of atmospheric NO_2 by pulsed cavity ring-down spectroscopy. *J. Geophys. Res.*, **111**, D12305, https://doi.org/10.1029/2005JD006942.

Pearson, G., F. Davies, and C. Collier, 2009: An analysis of the performance of the UFAM pulsed Doppler lidar for observing the boundary layer. *J. Atmos. Oceanic Technol.*, **26**, 240–250, https://doi.org/10.1175/2008JTECHA1128.1.

Rose, T., S. Crewell, U. Lehnert, and C. Simmer, 2005: A network suitable microwave radiometer for operational monitoring of the cloudy atmosphere. *Atmos. Res.*, **75**, 183–200, https://doi.org/10.1016/j.atmosres.2004.12.005.

Sathe, A., J. Mann, N. Vasiljevic, and G. Lea, 2015: A six-beam method to measure turbulence statistics using ground-based wind lidars. *Atmos. Meas. Tech.*, **8**, 729–740, https://doi.org/10.5194/amt-8-729-2015.

Sulzer, P., and Coauthors, 2014: A proton transfer reaction-quadrupole interface time-of-flight mass spectrometer (PTR-QiTOF): High speed due to extreme sensitivity. *Int. J. Mass Spectrom.*, **368**, 1–5, https://doi.org/10.1016/j.ijms.2014.05.004.

Wuttke, S., A. Kreuter, and M. Blumthaler, 2012: Aerosol climatology in an Alpine valley. *J. Geophys. Res.*, **117**, D20202, https://doi.org/10.1029/2012JD017854.

Yuan, B., A. R. Koss, C. Warneke, M. Coggon, K. Sekimoto, and J. A. de Gouw, 2017: Proton-transfer-reaction mass spectrometry: Applications in atmospheric sciences. *Chem. Rev.*, **117**, 132187–132229, https://doi.org/10.1021/acs.chemrev.7b00325.

Zhao, X., and Coauthors, 2019: Retrieval of total column and surface NO_2 from Pandora zenith-sky measurements. *Atmos. Chem. Phys.*, **19**, 10619–10642, https://doi.org/10.5194/ACP-19-10619-2019.